

Design, synthesis and anticancer activity of novel 4-(5-amino-4-cyano-1,3-oxazol-2-yl)benzenesulfonamide derivatives

Oleksandr Severin^a, Stepan Pilyo^a, Ivan Semenyuta^{b*}, Maryna Kachaeva^a, Victor Zhirnov^a and Volodymyr Brovarets^a

^aDepartment of chemistry of bioactive nitrogen-containing heterocyclic bases, V. P. Kukhar Institute of Bioorganic Chemistry and Petrochemistry, 02094, Kyiv, Ukraine

^bDepartment of chemistry of natural compounds, V. P. Kukhar Institute of Bioorganic Chemistry and Petrochemistry, 02094, Kyiv, Ukraine

CHRONICLE

Article history:

Received February 28, 2024

Received in revised form

March 31, 2024

Accepted August 13, 2024

Available online

August 13, 2024

Keywords:

1,3-oxazole

Anticancer agent

Sulfonamide

Estrogen receptor

ERα

ABSTRACT

Fourteen novel 4-(5-amino-4-cyano-1,3-oxazol-2-yl)benzenesulfonamides have been designed, synthesized, and characterized by spectroscopy and spectrometry methods. They have also been investigated on the NCI-60 cancer cell lines. The most activity compounds, **2**, **3**, and **9**, in concentration 10 μM demonstrated mean GI₅₀ values of 77, 70, and 68%, respectively, against the tumor cells. The best activity compound **2** showed the following GI₅₀ values: non-small cell lung cancer (HOP-92) - 4.56 μM, breast cancer (MDA-MB-468) - 21.0 μM, melanoma (SK-MEL-5) - 30.3 μM. Besides, this compound indicates low toxicity with TGI and LC₅₀ values >100 μM against all cancer cell lines. The COMPARE analysis (NCI) of compound **2** showed a very high correlation (r=0.91) with Tamoxifen as a selective estrogen receptors modulator. Molecular docking studies of ligand **2** demonstrated the complexation with estrogen receptors as a possible antitumor mechanism. The ADMET analysis of compound **2** indicates an optimistic prediction as an antitumor agent.

© 2025 by the authors; licensee Growing Science, Canada.

1. Introduction

Multidrug resistance to anticancer drugs used in tumor chemotherapy and associated side effects necessitate constant efforts to identify new, more effective drugs with improved anticancer activity and fewer side effects.^{1,2} Sulfonamides are bioisosteres of the carboxyl group because the distance between the oxygen atoms in these functional groups is approximately equal.^{3,4} The carboxylic functional group is widely used in drug design to functionalize various heterocyclic moiety anticancer agents. Moreover, molecules with the sulfonamide group demonstrate high pharmacological potential compared to ones with carboxylate functional groups due to their enhanced stability and biological activity.^{5,6} In medicinal chemistry, the bioisosterism of these groups is actively utilized to develop more effective drugs. So, a series of known sulfonamide-containing drugs have been successfully applied for cancer therapy and approved by the US FDA. Amsacrine is approved for treating acute leukemia and malignant lymphoma,⁷ Belinostat is used to treat T-cell lymphoma,⁸ and dabrafenib as BRAF inhibitor is employed to therapy metastatic melanoma and non-small cell lung cancer.⁹ Lung cancer is one of the leading causes of cancer death among men and women, with a 5-year survival rate of about 20% for lung cancer patients. Treatment of lung cancer is specific and depends on the type of cancer cells, the extent of spread, the health status of the patient, and depending on the mutations of the cancer cells, in particular EGFR inhibitors (osimertinib, erlotinib, gefitinib, afatinib), ALK inhibitors (crizotinib, alectinib, brigatinib, and ceritinib), MET inhibitors (capmatinib, tepotinib), BRAF inhibitor dabrafenib, ROS1 inhibitors crizotinib, lorlatinib, entrectinib.¹⁰ It is also necessary to note the combined antiproliferative effect of Tamoxifen and gefitinib on non-small cell lung cancer cells, as studied in the work.¹¹ Among them, oxazole derivatives are prominent, demonstrating various biological activities. So, oxazole-contained mubritinib is a known ERBB2 inhibitor with anti-leukemic activity.¹² However, in addition to resistance, all anticancer drugs have many

* Corresponding author Tel.: +38044573-26-55
E-mail address ivan@bpci.kiev.ua (I. Semenyuta)

disadvantages, such as drug interactions, contraindications, and selectivity of action. We previously synthesized 2-phenyl-1,3-oxazole-5-sulfonamide derivatives, which showed high anticancer activity *in vitro*.¹³ Compounds **3** and **5** showed high activity against lung cancer cells NCI-H522 with GI₅₀=0.278 - 0.465 μ M values. Also, they demonstrated low-level cytotoxicity with TGI \geq 100 μ M and LC₅₀ \geq 100 μ M about leukemia, ovarian, breast, and lung cancer cell lines. Therefore, the compounds in the present study have been further functionalized at the oxazole 5-position with piperidine, 4-methylpiperidine, and morpholine end-groups, which are characteristic of anticancer drugs such as gefitinib, olmutinib, dacomitinib (**Fig. 1**).

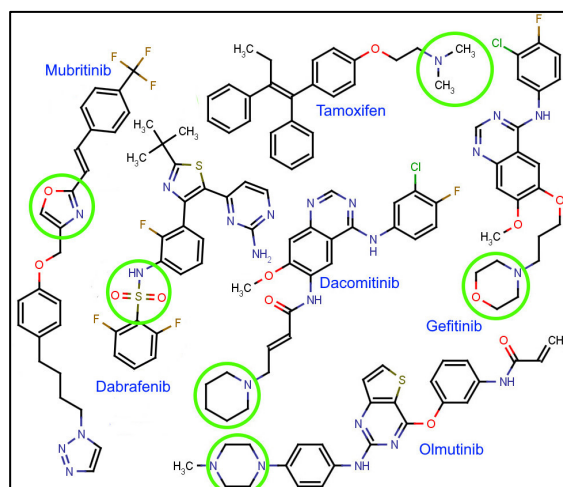


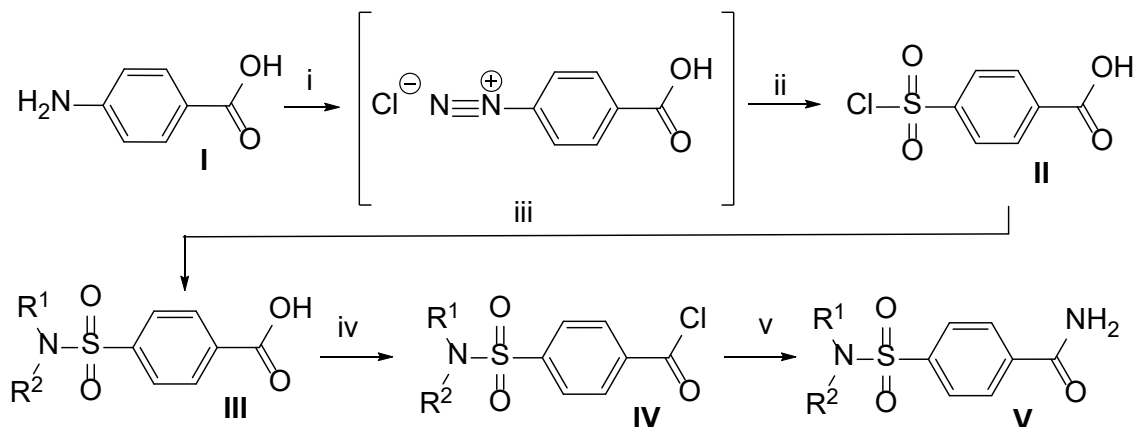
Fig. 1. Functional groups of nitrogen-containing US FDA-approved anticancer drugs.

Therefore, in our work, the 5-amino-2-phenyl-1,3-oxazole-4-carbonitriles were further modified by adding the *N,N*-dimethylbenzenesulfonamide or *N,N*-diethylbenzenesulfonamide or pyrrolidinebenzenesulfonamide groups in the 2nd position and morpholine, piperidine, piperazine, and pyrrolidine substituents in the 5-position of oxazole (**Table S1**). In addition, the potential molecular mechanisms of antitumor action and the pharmacokinetic properties of these compounds were investigated using NCI Compare analysis, molecular docking, and ADMET prediction.

2. Results and Discussion

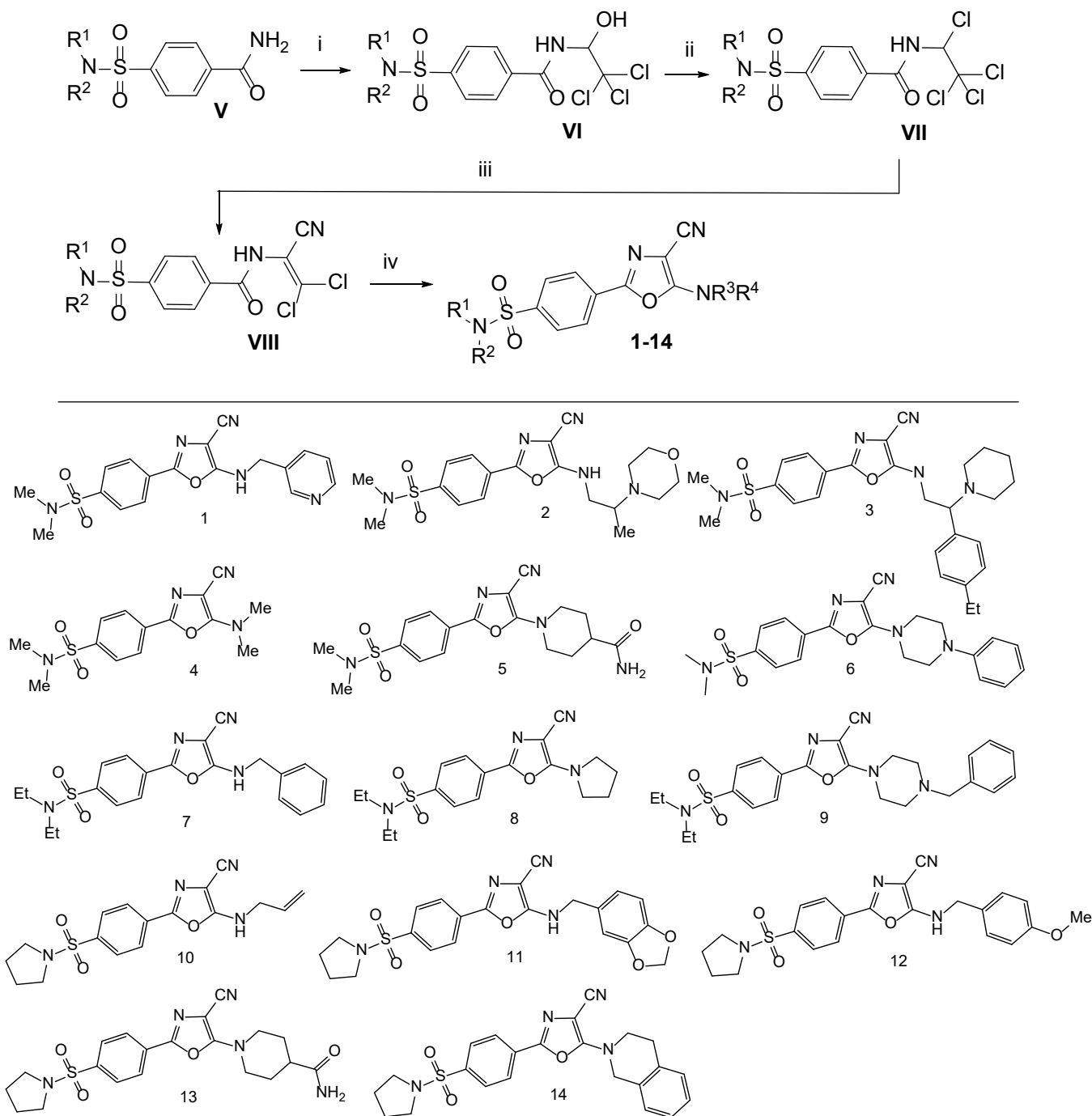
2.1. Chemistry

For a synthesis of 4-(5-amino-4-cyano-1,3-oxazole-2-yl)benzenesulfonamides **1-14** 4-(*N,N*-dialkylsulfamoyl)benzamides **V** were used as a starting compounds to obtain novel *N*-(2,2-dichloro-1-acrylonitrile)benzamides **VIII** and subsequent heterocyclization into compounds **1-14**. The compounds **V** were synthesized from corresponding sulfonyl chlorides **IV** obtained according to the general method presented in **Scheme 1**, which is described in the literature.¹⁴ The nitrosation of *p*-aminobenzoic acid **I** with nitrous acid (generated *in situ* from sodium nitrite and hydrochloric acid) followed by the reaction of obtained diazonium salt with sulfur dioxide in acetic acid solution lead to 4-(chlorosulfonyl)benzoic acid **II**¹⁴ converted to a 4-(dialkylsulfamoyl)benzoic acid **III**¹⁵⁻¹⁷ by reaction with aliphatic amines. By reacting compound **III** with thionyl chloride followed by reaction of obtained 4-(dialkylsulfamoyl)benzoyl chlorides **IV** with aqueous ammonia 4-(dialkylsulfamoyl)benzamides **V** were synthesized (**Scheme 1**).



Scheme 1. Synthesis of 4-(dialkylsulfamoyl)benzamides **V**. Reagents and conditions: i: NaNO₂, HCl, -10 °C; ii: SO₂ / MeC(O)OH, -5-0 °C; iii: NHR¹R², Et₃N; iv: S(O)Cl₂, reflux 3-5 h; v: NH₃ aq. 0-10 °C.

Compounds **V** were used for the synthesis of enamides **VIII** – key compounds for the obtaining of oxazoles **1-14**. The synthesis of 4-sulfonylamide-*N*-(2,2-dichloro-1-acrylonitrile)benzamides **VIII** was carried out in several stages.¹⁸ By the reaction of 4-(*N,N*-dialkylsulfamoyl)benzamides **V** with chloral hydrate in the presence of concentrated sulfuric acid 4-(*N,N*-dialkylsulfamoyl)-*N*-(2,2,2-trichloro-1-hydroxyethyl)benzamides **VI** were obtained. Compounds **VI** were converted into 4-(*N,N*-dialkylsulfamoyl)-*N*-(1,2,2,2-tetrachloroethyl)benzamides **VII** by reacting **VI** with thionyl chloride. Transformation **VII**→**VIII** was carried out by cyanation at -10-0 °C. Synthesized enamides **VIII** were used to obtain 4-(5-amino-4-cyano-1,3-oxazole-2-yl)benzene-sulfonamides **1-14** (**Scheme 2**). The method of synthesis of compounds **1-14** by cyclization of 2,2-dichloroenamides **VIII** with secondary amines was described in the work.¹⁸ Reaction is carried out in the presence of excess of triethylamine at 20-25 °C.



Scheme 2. Synthesis of 4-(5-amino-4-cyano-1,3-oxazole-2-yl)-benzenesulfonamides **1-14**. Reagents and conditions: i: Cl₃CC(O)H*H₂O, H₂SO₄ (c), heating; ii: S(O)Cl₂, C₆H₆, reflux 3-5 h; iii: 2KCN, H₂O -10-0 °C, 3-5 h; iv: NHR³R⁴, 2,2Et₃N, 20-25 °C, 12 h.

The IR, ¹H ¹³C NMR, and LCMS spectra confirmed the structures of synthesized compounds. All spectral data are summarized in the Supplementary materials (**Fig.S1–S68**). All aromatic and aliphatic proton signals are visible in the ¹H NMR spectrum. The ¹H NMR signal of the NH group of compounds **1-3**, **7**, **10-12** appeared as a singlet or triplet at 9.23-8.44 ppm. The ¹³C NMR signals of the C4 and C5 of 1,3-oxazole ring are good visible at 86.6-77.4 ppm (C4) and 162.2-

159.0 ppm (C5) ppm. Intensive absorption bands in the IR spectra of the SO₂-group appeared at 1343–1328 cm⁻¹ and 1168–1155 cm⁻¹, of CN – at 2214–2201 cm⁻¹, NH (compounds **1-3**, **7**, **10-12**) – at 3430–3086 cm⁻¹. In the IR spectra two intense absorption bands characteristic of 5-amino-1,3-oxazoles are visible in the region of 1635–1580 cm⁻¹^{18,19} confirming the presence of an oxazole ring in the molecule. The molecular ion peaks (LCMS data) of the compounds **1-14** are responded to molecular ions of substances.

2.2. Biology, SAR and COMPARE analysis

2.2.1. The one-dose assay for all compounds.

The synthesized novel 4-(5-amino-4-cyano-1,3-oxazol-2-yl)benzenesulfonamide compounds (**1-14**) were investigated on anticancer activity in the 10⁻⁵ M concentration against NCI-60 cancer cell lines (**Table S2**). The results demonstrate most activity compounds **2**, **3**, and **9** with mean values GI = 77, 70, and 68%, respectively (**Table 1**).

Table 1. Anticancer activity for all compounds against NCI-60 cancer cell lines

Comp.	GI values for all panels (mean), %	Average GI values, %	Best sensitive NCI-60 cell line	GI for best sensitive cell line, %
1	100.07	66.18 - 123.66	NSCLC/ HOP-92/	66.18
2	77.09	-94.07 - 127.37	Melanoma/ LOX IMVI	-94.07
3	70.38	28.85 - 131.53	Breast cancer/ MDA-MB-468	28.85
4	102.28	81.80 - 120.69	Leukemia/ HL-60(TB)	81.80
5	98.34	68.32 - 122.64	Melanoma/ SK-MEL-5	68.32
6	87.99	38.41- 117.65	Melanoma/ SK-MEL-5	38.14
7	99.41	47.06 - 116.14	Melanoma/ SK-MEL-5	47.06
8	96.82	56.11 - 132.12	Melanoma/ SK-MEL-5	56.11
9	67.79	7.11 - 105.28	Breast cancer/ MDA-MB-468	7.11
10	103.26	84.05 - 139.99	CNS cancer/ SNB-19	84.05
11	94.91	29.67 - 119.99	CNS cancer/ SNB-75	29.67
12	99.71	43.90 - 120.24	CNS cancer/ SNB-75	43.90
13	104.65	84.05 - 132.65	Breast cancer/ MCF7	84.05
14	100/96	81.41 - 140.66	Leukemia/ K-562	81.41

Table 2. Growth inhibition of a series of tumor cells by compounds **2**, **3**, and **9**.

Cancer cells/ subpanel	Compounds/ GI, %		
	2	3	9
Leukemia			
K-562	11	66	81
RPMI-8226	A ¹	62	73
HL-60 (TB)	0	47	51
MOLT-4	A	45	55
SR	n/d ²	43	51
Lung cancer			
EKVX	82	39	46
NCI-H226	87	34	34
NCI-H23	101	35	35
HOP-92	n/d	56	24
Colon cancer			
HCC-2998	192	14	11
HCT-15	123	48	38
HCT-116	A	50	42
CNS			
SF-295	84	37	43
Melanoma			
LOX IMVI	194	21	18
SK-MEL-5	173	60	94
SK-MEL-2	A	4	50
MDA-MB-435	A	17	74
Ovarian cancer			
NCI/ADR-RES	76	45	36
Renal cancer			
RXF 393	121	58	20
Prostate cancer			
PC-3	A	62	50
Breast cancer			
MCF7	107	44	35
MDA-MB-468	134	71	93

¹ The compound activates growth cells; ² no data.

The remaining compounds show minimal mean inhibition across all cell lines. Notably, for inactive compounds **1**, **4-8**, and **10-14**, it is characteristic of point inhibition of some cancer cells. So, compounds **5-8** inhibit melanoma cancer cells

SK-MEL-5 (GI = 32-62%), and compounds **10-12** are characterized by inhibition of CNS cancer cells SNB-19 and SNB-75 with GI values of 16 - 71%; compound **1** inhibits growth the lung cancer cells HOP-92 on 34%; compounds **4 - 14** inhibit the growth of leukemia cancer cells (K-562 and HL-60(TB) on 18-19 % and compound **13** show GI=16 % for breast cancer cells MCF7. Complete data results from the NCI-60 one-dose assay for all synthesized compounds are presented in **Table S2**. Next, we will examine in detail the anticancer activity of compounds **2, 3, and 9**.

Compounds **2, 3, and 9** inhibited the growth of 12, 8, and 11 cell lines from the total panel by >50%, respectively (**Table 2**). Compound **2** showed cytostatic and cytotoxic activity against 12 cell lines. The mean activity of compounds **2, 3, and 9**, calculated from the percentage of cell growth inhibition against sensitive lines, was 120±13, 62±2, and 66±5%, respectively. The compound **2** demonstrates the greatest inhibition activity for the following NCI-60 cancer cell lines: melanoma cancer cells – LOX IMVI (GI=192%) and SK-MEL-5 (GI=173%); colon cancer cell line HCC-2998 (GI=192%) and HST-15 (GI=123%); breast cancer cell lines MCF7 and MDA-MB-468 with values GI=107, 134% respectively; renal cancer cell line RFX-393 (GI=121%). Also, compound **2** shows growth inhibition in lung cancer cells NCI-H23 (GI=101%), NCI-H226 (GI=87%), EKVX (GI=82%), and CNS cancer cell SF-295 with GI=84%. It should also be noted that compound **2** did not inhibit leukemia cell lines, unlike compounds **3 and 9** (GI= 43 - 81%), which may be due to structural features of compounds.

2.2.2. Structure-activity relationship

The SAR study of the most activity compounds **2, 3, and 9** showed that the 5-position of oxazole replacement of the compound **2** morpholine group to piperidine or piperazine group reduced the number of sensitive cell lines in compounds **3 and 9**. At the same time, compound cytotoxicity was decreased, and the spectrum of antitumor activity changed. It should be noted that compounds **3 and 9** showed moderate (50% ≥ GI < 70%) and high (70% ≤ GI < 90%) activity, respectively, against leukemia cell lines. In contrast, compound **3** did not show any activity against the CNS cancer and ovarian cancer cell lines but demonstrated moderate activity against prostate cancer cell line PC-3, and compound **9** was active exclusively against leukemia, melanoma, and breast cancer cell lines. Next, compound **2** anticancer activity was investigated in more detail using an NCI-60 five-dose assay.

2.2.3. The five-dose assay for compound 2

The results of compound **2** anticancer activity (**Fig. S69**) demonstrate cell growth inhibition in the micromolar range ($10^{-4} - 10^{-6}$ M) for non-small cell lung cancer cells (HOP-92 and NCI-H226) with GI₅₀ values of 4.56 μM and 81.80 μM, respectively. It was also noted that growth inhibition breast cancer cell lines MDA-MB-468 – GI₅₀=21.0 μM, BT-549 – GI₅₀=67.80 μM, and T-47D cell line – GI₅₀=97.50 μM. In addition, growth inhibition was observed on leukemia cells K-562 (GI₅₀=45.30 μM), SR (GI₅₀=60.40 μM), MOLT-4 (GI₅₀=85.80 μM), and RPMI-8226 (GI₅₀=94.80 μM). Moreover, growth inhibition shows melanoma cells SK-MEL-5 with GI₅₀ – 30.30 μM, ovarian cancer cells OVCAR-4 with GI₅₀ – 93.30 μM, and renal cancer cell line RFX 393 (GI₅₀=77.80 μM) (**Table 2**).

Table 2. Results of anticancer activity of compound **2** against a row NCI-60 human cancer cell lines.

Panel/Cell lines	GI ₅₀ , μM	TGI, μM	LC ₅₀ , μM
Leukemia			
K-562	45.30		
MOLT-4	85.80	> 100	>100
RPMI-8226	94.80		
SR	60.40		
Non-Small Cell Lung Cancer			
HOP-92	4.56	> 100	>100
NCI-H226	81.8		
Melanoma			
SK-MEL-5	30.3	> 100	>100
Ovarian Cancer			
OVCAR-4	93.3	> 100	>100
Renal Cancer			
RFX 393	77.8	> 100	>100
Breast Cancer			
BT-549	67.8		
T-47D	97.5	> 100	>100
MDA-MB-468	21.0		

Therefore, the compound **2** five-dose results indicate the greatest antitumor activity relative to non-small cell lung cancer (GI₅₀=4.56 μM), breast cancer (GI₅₀=21.0 μM), and melanoma – 30.3 μM. It should be emphasized that compound **2** demonstrates low cytotoxicity for all NCI-60 cancer cell lines with values TGI and LC₅₀ >100 μM. Further, compound **2** was studied for the potential molecular mechanism of antitumor action.

2.3. Molecular modelling

2.3.1. COMPARE analysis

We used the COMPARE analysis to study compound **2**'s potential molecular mechanism of anticancer activity. This approach measures the similarity of compound **2**'s antitumor activity with the standard anticancer agents (GI_{50}) in the NCI DTP database. The results of the COMPARE correlation are shown in **Fig. 2**.

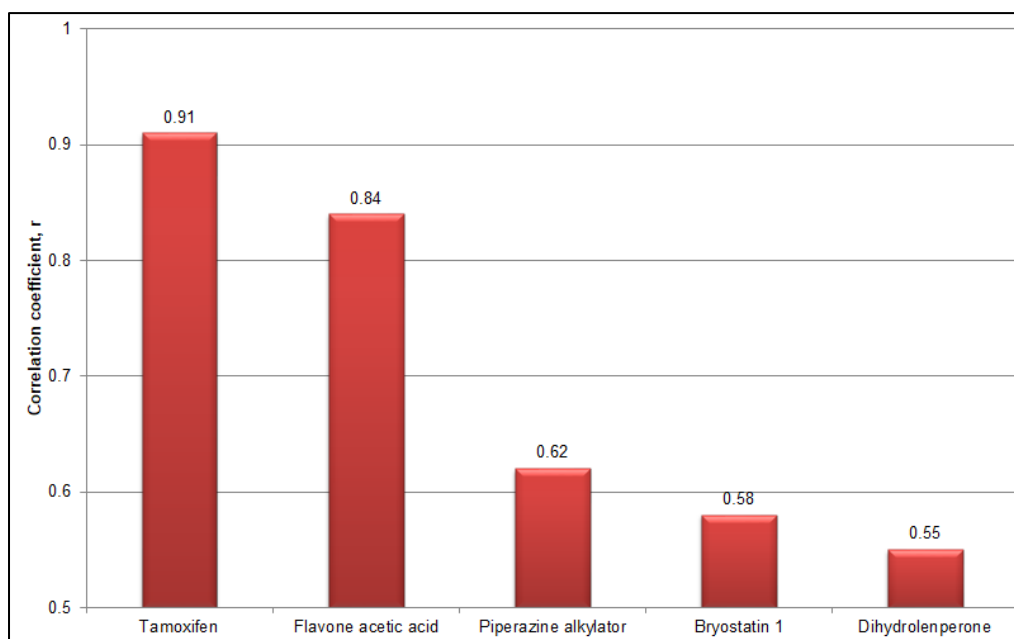


Fig. 2. The COMPARE correlation results for compound **2** by GI_{50} vector.

Compound **2** demonstrated a very high correlation ($r=0.91$) with Tamoxifen and flavone acetic acid ($r=0.84$) and a strong and medium coefficient correlation with piperazine alkylator ($r=0.62$), Bryostatin 1 ($r=0.58$), and Dihydrolenperone ($r=0.55$) (**Fig. 2**). These antitumor agents' molecular mechanism of action consists of Tamoxifen is a selective estrogen receptor modulator; flavone acetic acid has immunomodulation action; the piperazine alkylator is an alkylating anticancer agent; Bryostatin 1 is a modulator of protein kinase C and Dihydrolenperone has antineoplastic activity. Thus, the most significant correlation ($r=0.91$) between the mean graph GI_{50} vector of compound **2** and Tamoxifen. One of the main functions of Tamoxifen is to suppress cancer cell proliferation triggered by signaling pathways associated with the estrogen receptor (ER).¹³ There are many molecular mechanisms underlying the action of ER on the proliferation, migration, and invasion of lung cancer cells. ER α in lung cancer has been observed mainly in the cytoplasm and has lived associated with poor prognosis. ER β appears to be the predominant form of lung large-cell adenocarcinoma. ER β expression is observed in the cytoplasm, nucleus, and mitochondria. Mitochondrial ER β inhibits Bcl-2-related protein Bad (promoter of apoptosis) and, respectively, Bad-Bcl-XL and Bad-Bcl-2 interactions suppressing apoptosis.²⁰ Besides, Tamoxifen also exerts anticancer effects in various cancer cell types through mitochondrial dysfunction by triggering cytochrome C release and activating caspase family proteins, inducing apoptosis.²¹⁻²³ It is essential to mention that the HOP-92 adenocarcinoma cell line has a balanced pro-oxidative state, with more antioxidant enzyme activity, fewer sulfhydryl groups, less antioxidant potential, and more lipoperoxidation and reactive species production.²⁴ Therefore, by disrupting this balance, Tamoxifen renders cancer cells vulnerable to apoptosis. Thus, based on COMPARE analysis data, a high correlation is observed between compound **2** and Tamoxifen. Hence, it can be assumed that compound **2**'s molecular targets are similar to Tamoxifen's. Furthermore, compound **2** has similar potency against the HOP-92 cell line ($GI_{50} = 4.53 \mu\text{M}$) compared to Tamoxifen ($GI_{50} = 2.50 \mu\text{M}$). Next, we investigated the possible mechanism of compound **2**'s anticancer activity by molecular modeling.

2.3.2. Comparison of molecular docking of ligands **2**, **3**, and **9** in the active sites of estrogen receptors α and β .

Compounds **2**, **3**, and **9** were modelled using structures of human estrogen receptor- α PDB ID: 5W9C, 1A52, and estrogen receptor- β PDB ID: 1QKN, 5TOA, obtained from the RCSB Protein Data Bank.²⁵ The co-crystallized ligands were utilized as docking centers. **Table 3** presents compounds **2**, **3**, and **9** docking results and redocking 4-hydroxytamoxifen, raloxifene, and estradiol in the active sites of ER α and ER β .

Table 3. The molecular docking characteristics of the ligands **2**, **3**, and **9** and redocking results

Compounds	ER α		ER β	
	ΔG , kcal/mol	Hydrogen bonds	ΔG , kcal/mol	Hydrogen bonds
2	-9.7	4	-8.0	3
3	-8.4	3	-8.5	2
9	-8.9	3	-8.2	2
4-hydroxytamoxifen	-10.2 ^a	4	-	-
Raloxifen	-	-	-11.0 ^a	3
Estradiol	-10.8 ^a	3	-11.2 ^a	3

^a based on redocking results.

The redocking of 4-hydroxytamoxifen, raloxifene, and estradiol in the active sites of human ERs shows estimated binding energy from -10.2 to -11.2 kcal/mol and the RMSD values for all atoms 1.32- 0.94 Å. The docking results show the formation of ligand-receptor complexes of compounds **2**, **3**, and **9** with ER α , with estimated binding energies ranging from -8.4 to -9.7 kcal/mol and forming 3 - 5 hydrogen bonds. Complexation compounds with ER β occur with lower energies from -8.0 to -8.5 kcal/mol and the formation of 2 - 3 hydrogen bonds. Thus, the most energetically favorable complexation was observed for compound **2** in the active site of ER α with $G = -9.7$ kcal/mol, which is correlated to high experimental anticancer activity and comparable with a binding energy of 4-hydroxytamoxifen (-10.2 kcal/mol) and estradiol (-10.8 kcal/mol). Next, **Fig. 3** shows feature of the complex formation of most activity ligand **2** in the ER α active site.

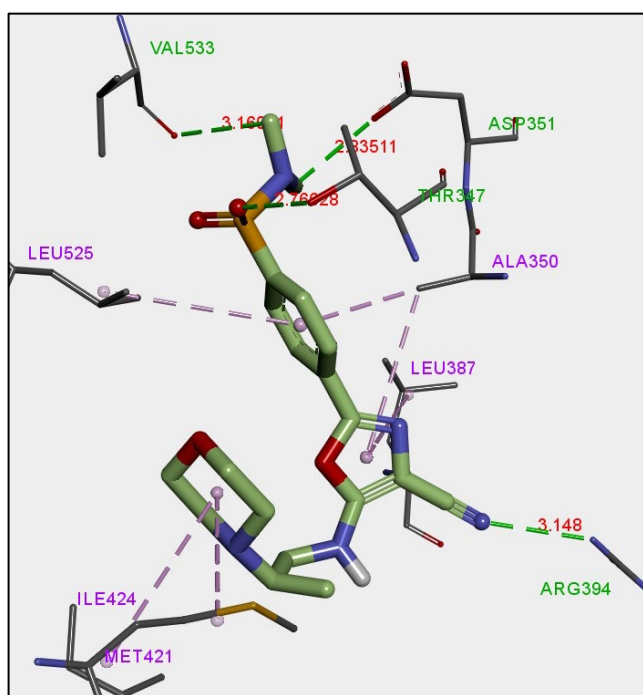


Fig. 3. Molecular docking of compound **2** into the active site of ER α .

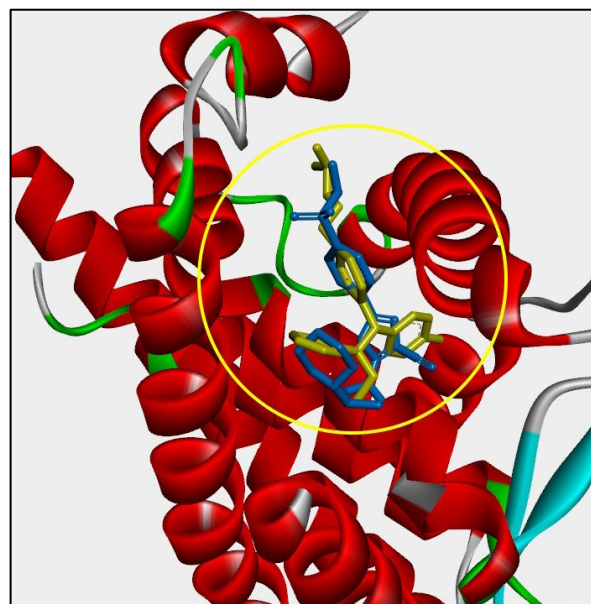


Fig. 4. Comparative position of 4-hydroxytamoxifen and ligand **2** docking position into the human ER α active site; yellow – 4-hydroxytamoxifen; blue – ligand **2**.

The formation of the ligand-protein complex is stabilized by four hydrogen bonds (2.33 - 3.14 Å) with the amino acids of the active site ER α (**Fig. 3**). So, the sulfonamide and carbonitrile group of compounds **2** forms three hydrogen bonds with the amino acids ASP351 (2.33 Å), THR347 (2.76 Å), VAL533 (3.16 Å), and ARG394 (3.14 Å), respectively. In addition, ligand two forms six hydrophobic interactions (3.61 - 5.20 Å) between the amino acid residues ALA350, LEU387, MET421, ILE424, LEU525, and phenyl, oxazole, morpholine rings. It should be noted that the hydrogen bond formation with the amino acids ASP351, THR347, VAL533, and ARG394 and hydrophobic interactions in the ER α active site take place similar to 4-hydroxytamoxifen and estradiol in the crystal structures of human estrogen receptor- α PDB ID: 5W9C and 1A52. To confirm, **Fig. 4** demonstrates the comparative localization of the co-crystallized modulator of ER α 4-hydroxytamoxifen and the docking position of ligand **2** in the human ER α active site.

Thus, studying the antitumor mechanism of compound **2** action by molecular docking suggests estrogen receptors as potential biotarget. The complexation of compound **2** in the active site of the ER α and ER β is happening with the predicted

binding energy values -9.7 and -8.0 kcal/mol, respectively. Stabilization of the ligand-receptor complex happens using the hydrogen bonds of the carbonitrile (oxazole ring) and sulfonamide groups with amino acids ARG394 (3.14 Å), ASP351 (2.33 Å), THR347 (2.76 Å), and VAL533 (3.16 Å). The molecular docking analysis of 4-(5-amino-4-cyano-1,3-oxazol-2-yl)benzenesulfonamide derivatives demonstrated a probable mechanism of the anticancer action via complexation with ER α , similar to Tamoxifen and other ER's modulators. Thus, designed and synthesized compounds can be used in drug design as ER modulators for treating estrogen-dependent tumors. Further, ADMET-related properties of compounds **2**, **3**, and **9** were investigated and compared to Tamoxifen.

2.3.3. ADMET evaluation.

Table 4 presents the calculated ADMET- properties of compounds **2**, **3**, and **9** by the pkCSM web platform, such as absorption, distribution, metabolism, excretion, and toxicity compared to the antitumor drug Tamoxifen. The compounds predicted absorption results show good water solubility, medium intestinal absorption (>76%), and Caco-2 assay permeability (0.7-0.9), which suggested good oral bioavailability. The distribution of compounds **2**, **3**, and **9** has a low permeability via the blood-brain barrier and effects on CNS. The compound metabolism results can be a substrate for cytochrome P450 and biotransforming by the main enzyme CYP3A4. The excretion of compounds also displayed low total clearance, similar to Tamoxifen. The indicated compounds' toxicity will have a low maximum tolerated dose and a low oral rate of acute and chronic toxicity comparable to Tamoxifen. The studied compounds predicted not to call skin sensitization.

Table 4. Comparative the pharmacokinetics and toxic characteristics of compounds **2**, **3**, **9**, and Tamoxifen

ADMET Parameters	Compounds			
	2	3	9	Tamoxifen
Molecular properties				
Molecular weight	419.507	509.632	479.606	371.524
LogP	1.59618	3.51138	3.56598	5.9961
H-acceptor	8	8	7	2
H-donor	1	1	0	0
Surface area	170.482	211.905	200.636	168.649
Absorption				
Water solubility (lg mol/L)	-2.856	-3.817	-4.614	-5.929
Intestinal absorption % (human)	76.62	84.369	96.882	96.885
Caco2 permeability	0.069	0.74	0.936	1.065
Distribution				
BBB permeability (lg BB)	-1.155	-1.133	-1.026	1.329
CNS permeability (log PS)	-3.108	-2.681	-2.573	-1.473
Metabolism				
CYP2D6 substrate	No	No	No	No
CYP3A4 substrate	Yes	Yes	Yes	Yes
Excretion				
Total clearance	0.623	0.698	0.295	0.556
Renal OCT2 substrate	Yes	Yes	Yes	No
Toxicity				
Max. tolerated dose (human)	0.113	0.387	-0.215	0.313
Oral rate acute toxicity (LD50) (mol/kg)	2.159	2.477	2.803	2.285
Oral rate chronic toxicity (LOAEL) (lg)	0.873	1.209	1.283	0.41
Skin sensitization	No	No	No	No

3. Conclusions

Fourteen novel 4-(5-amino-4-cyano-1,3-oxazol-2-yl)-benzenesulfonamides were designed, synthesized with 65-90% yields, modified with various substituents, and described. The anticancer activity of these compounds has been conducted by the NCI-60 cell line panels in the one-dose (compound **2** to five-dose) assays. The five-dose assay results of compound

2 demonstrate cell growth inhibition (GI₅₀) in non-small cell lung cancer (4.56 μM and 81.80 μM), breast cancer cells (21.0 μM, 67.80 μM, and 97.50 μM), leukemia cells (45.30 μM, 60.40 μM, 85.80 μM, and 94.80 μM), melanoma cancer cells (30.30 μM), ovarian cancer cells (93.30 μM), and renal cancer cell (77.80 μM). The COMPARE analysis demonstrated a very high correlation (r=0.91) of compound **2** (GI₅₀ vector) with Tamoxifen, a known selective estrogen receptor modulator. The SAR analysis of synthesized compounds showed that the presence of the morpholine moiety at the C5 position of an oxazole is critical since the addition of the phenyl, piperidine, and piperazine groups reduces the anticancer activity of these compounds. The molecular docking analysis demonstrated the probable anticancer mechanism action of compound **2** as an ER modulator. The ADMET properties acknowledged the favorable prognosis using compounds as antitumor agents. Thus, the results of this study allow compound **2** as the basis for further modification to obtain derivatives as ER modulators for treating estrogen-dependent tumors.

Supporting Information Summary

The Supporting Information contains NCI results for the anticancer activity of compounds **1-14** and IR, ¹H, ¹³C, ³¹P NMR, and LC/MS spectra of the compounds.

Acknowledgments

We thank the National Cancer Institute, Bethesda, MD, USA, for the in vitro evaluation of anticancer activity within the Developmental Therapeutic Program and Enamine Ltd for the material and technical support. This work was supported by the National Academy of Sciences of Ukraine under Grants of the NAS of Ukraine to research laboratories/groups of young scientists of the NAS of Ukraine to conduct research in the priority directions of the development of science and technology in 2024-2025 "Novel synthetic nitrogen-containing heterocyclic compounds with antimicrobial and anticancer activity" (Contract №29/02-2024(5) from 19.02.2024).

Conflict of Interests

The authors declare that there is no conflict of interest regarding the publication of this paper.

4. Experimental

4.1. Chemistry

General. Commercially available chemical reagents and solvents were purchased and used without purification. The TLC method was applied to monitor the reaction progress. ¹H and ¹³C NMR spectra were recorded in DMSO-d₆ on a Varian Mercury spectrometer using the signal of residual solvent protons as an internal standard. IR spectra were recorded on a Vertex-70 spectrometer in KBr tablets. LCMS spectra were obtained using an Agilent 1200 Series high-performance liquid chromatograph. Fisher-Johns apparatus was used for the melting point determination.

Synthesis of 4-(chlorosulfonyl)benzoic acid II was carried out according to a literature method ¹⁴ starting from available *p*-aminobenzoic acid **I**.

Compounds **III** (4-(dimethylsulfamoyl)benzoic acid ¹⁵, 4-(diethylsulfamoyl)benzoic acid ¹⁶, 4-pyrrolidin-1-ylsulfonylbenzoic acid ¹⁷ and its synthesis were described previously.

Synthesis of 4-(dialkylsulfamoyl)benzoyl chlorides IV. To a suspension of 0.3 mol of corresponding 4-(dialkylsulfamoyl)benzoic acid **III** in 100-150 ml of anhydrous dioxane, 0.35 mol of thionyl chloride was added. The reaction mixture was heated to 80-90 °C (oil bath temperature) for 2-3 h until the gas evolution stopped, then it was cooled to 20-25 °C, and the solvent was evaporated under vacuum. The residue was treated with anhydrous hexane, the precipitate was filtered, dried in vacuum and obtained products **IV** were used for the next stage.

Synthesis of 4-(dialkylsulfamoyl)benzamides V. Solution of 0.1 mol of corresponding 4-(dialkylsulfamoyl)benzoyl chloride **IV** in 40 ml of anhydrous dioxane was added dropwise to solution of 200.0 ml of aqueous ammonia 25% at 0°C for 0.5 h. The mixture was stirred at 0°C for 2 h. The precipitate was filtered off, dried, and obtained products **V** were used for the next stage.

Synthesis of 4-(N,N-dialkylsulfamoyl)-N-(2,2,2-trichloro-1-hydroxyethyl)benzamides VI. 0.1 Mol of corresponding 4-(dialkylsulfamoyl)benzamides **V**, 0.12 mol of chloral hydrate and 2 ml of conc. sulfuric acid were heated in a water bath to an exothermic reaction. After its initiation, the mixture was continued to be heated with intense stirring for another 1 h, then cooled to 20-25°C, treated with an excess of water, the precipitate was filtered, dried in air, and obtained products **VI** were used for further syntheses.

Synthesis of 4-(N,N-dialkylsulfamoyl)-N-(1,2,2,2-tetrachloroethyl)-benzamides VII. To a suspension of 0.1 mol of compound **VI** in 100 ml of benzene, 0.11 mol of thionyl chloride was added. The reaction mixture was heated, to 80-90 °C (oil bath temperature) for 2-3 h until the gas evolution stopped, then it was cooled to 20-25°C and the solvent was evaporated under vacuum. The residue was treated with anhydrous hexane, the precipitate was filtered and obtained products **VII** were used for the next stage.

The synthesis of 4-sulfonylamide-*N*-(2,2-dichloro-1-acrylonitrile)benzamides **VIII**. A saturated solution of 0.1 mol of the corresponding product VII in anhydrous dioxane (70 ml) was added dropwise over 0.5 h to a solution of 0.2 mol of potassium cyanide in 100 ml of water with vigorous stirring and cooling to -10 °C. The mixture was stirred for 2 h at -10 °C, and then for 2 h at -5 °C, and at room temperature for 2-3 h. The reaction mixture was poured with water, the precipitate was filtered off, washed with a small amount of water, dried at 20-25 °C in the air, and recrystallized from acetonitrile.

N-(2,2-Dichloro-1-cyanoethenyl)-4-(dimethylsulfamoyl)benzamide **VIIIa**. Yield, 89%; M.p. 211-213 °C (MeCN); IR (KBr) ν cm⁻¹: 3324 (NH), 2225 (CN), 1694, 1595, 1500, 1477, 1455, 1329 (SO₂), 1314, 1299, 1260, 1182, 1163 (SO₂), 1113, 1088, 1055, 1012, 960, 921, 766, 756, 707, 687, 649, 593, 538. ¹H NMR (400 MHz, DMSO-d₆) δ 11.00 (s, 1H), 8.18 (d, *J* = 8.1 Hz, 2H), 7.93 (d, *J* = 8.1 Hz, 2H), 2.65 (s, 6H). ¹³C NMR (126 MHz, DMSO-d₆) δ : 164.3, 138.3, 135.5, 135.1, 129.0, 127.8, 112.7, 110.7, 37.5. LC/MS, *m/z*: 348.2 [M+1]⁺.

N-(2,2-Dichloro-1-cyanoethenyl)-4-(diethylsulfamoyl)benzamide **VIIIb**. Yield, 90%; M.p. 180-182 °C (MeCN); IR (KBr) ν cm⁻¹: 3253 (NH), 2231, 2219 (CN), 1669, 1633, 1598, 1506, 1481, 1470, 1363, 1336 (SO₂), 1306, 1299, 1200, 1159, 1120 (SO₂), 1086, 1015, 970, 923, 853, 766, 757, 696, 649, 616, 596, 560. ¹H NMR (400 MHz, DMSO-d₆) δ 10.94 (s, 1H), 8.11 (d, *J* = 8.1 Hz, 2H), 7.98 (d, *J* = 8.1 Hz, 2H), 3.20 (q, *J* = 7.1 Hz, 4H), 1.05 (t, *J* = 7.1 Hz, 6H). ¹³C NMR (126 MHz, DMSO-d₆) δ 164.3, 143.4, 135.1, 135.0, 129.1, 127.0, 112.7, 110.7, 41.8, 14.0. LC/MS, *m/z*: 376.2 [M+1]⁺.

N-(2,2-Dichloro-1-cyanoethenyl)-4-(pyrrolidin-1-ylsulfamoyl)benzamide **VIIIc**. Yield, 85% (beige solid); M.p. 210-212 °C (MeCN). IR (KBr) ν cm⁻¹: 3308 (NH), 3283 (NH), 2224 (CN), 1693, 1595, 1502, 1478, 1333 (SO₂), 1313, 1296, 1258, 1162 (SO₂), 1109, 1090, 1008, 923, 654, 602, 581. ¹H NMR (400 MHz, DMSO-d₆) δ 10.95 (s, 1H), 8.14 (d, *J* = 8.0 Hz, 2H), 7.99 (d, *J* = 8.0 Hz, 2H), 3.17 (t, *J* = 8.0 Hz, 4H), 1.67-1.64 (m, 4H). ¹³C NMR (126 MHz, DMSO-d₆) δ 164.31, 139.77, 135.37, 135.06, 129.03, 127.58, 112.70, 110.67, 47.84, 24.73. LC/MS, *m/z*: 374.2 [M+1]⁺.

Synthesis of 4-(5-amino-4-cyano-1,3-oxazole-2-yl)-benzenesulfonamides **1-14**.²⁶ 0.001 Mol of the corresponding amine and 0.001 mol of triethylamine were added to a solution of 0.001 mol of one of the 4-sulfonylamide-*N*-(2,2-dichloro-1-acrylonitrile)benzamides **VIIIa-c** in anhydrous dioxane (30 ml), the mixture was boiled for 2 h, left at 20-25 °C for 12 h, the precipitate was filtered, the solvent was removed *in vacuo*, the residue was treated with water, filtered, dried, and compounds **1-14** were purified by recrystallization from EtOH or MeCN.

4-[4-Cyano-5-(pyridin-3-ylmethylamino)-1,3-oxazol-2-yl]-*N,N*-dimethylbenzenesulfonamide **1**. Yield, 77% (colorless solid); M.p. 204-206 °C (EtOH); IR (KBr) ν cm⁻¹: 3364 (NH), 2207 (CN), 1627, 1603, 1575, 1478, 1454, 1427, 1405, 1336 (SO₂), 1319, 1287, 1259, 1180, 1160 (SO₂), 1090, 1043, 1027, 947, 834, 773, 739, 709, 698 683, 611, 594, 569, 541. ¹H NMR (400 MHz, DMSO-d₆) δ 9.24 (s, 1H), 8.66 (s, 1H), 8.53 (d, *J* = 4.0 Hz, 1H), 8.03 (d, *J* = 12.0 Hz, 2H), 7.86 (d, *J* = 12.0 Hz, 2H), 7.83 (br s, 1H), 7.43-7.40 (m, 1H), 4.64 (s, 2H), 2.64 (s, 6H). ¹³C NMR (126 MHz, DMSO-d₆) δ 161.3 (C5_{oxazole}), 158.5, 148.9, 148.8, 148.3, 135.3, 133.4, 129.4, 128.4, 125.7, 123.7, 115.1, 84.9 (C4_{oxazole}), 43.8, 37.5. LC/MS, *m/z*: 384.4 [M+1]⁺.

4-[4-Cyano-5-(2-morpholin-4-ylpropylamino)-1,3-oxazol-2-yl]-*N,N*-dimethylbenzenesulfonamide **2**. Yield, 67% (colorless solid); M.p. 177-179 °C (EtOH); IR (KBr) ν cm⁻¹: 3328 (NH), 3086, 2974, 2820, 2214 (CN), 1626, 1602, 1579, 1478, 1455, 1339 (SO₂), 1168 (SO₂), 1150, 1117, 1089, 1055, 950, 854, 761, 749, 701, 610, 586, 550. ¹H NMR (400 MHz, DMSO-d₆) δ 8.49 (s, 1H), 8.02 (d, *J* = 8.0 Hz, 2H), 7.85 (d, *J* = 8.0 Hz, 2H), 3.53-3.46 (m, 5H), 3.24-3.21 (m, 1H), 2.81-2.74 (m, 1H), 2.64 (s, 6H), 2.59-2.40 (m, 4H), 0.99 (d, *J* = 8.0 Hz, 3H). ¹³C NMR (126 MHz, DMSO-d₆) δ 161.9 (C5_{oxazole}), 147.8, 135.2, 129.5, 128.4, 125.5, 115.6, 84.3 (C4_{oxazole}), 66.6, 58.6, 48.5, 45.3, 37.5, 11.5. LC/MS, *m/z*: 420.0 [M+1]⁺.

4-[4-Cyano-5-[[2-(4-ethylphenyl)-2-piperidin-1-ylethyl]amino]-1,3-oxazol-2-yl]-*N,N*-dimethylbenzenesulfonamide **3**. Yield, 69% (colorless solid); M.p. 145-147 °C (EtOH); IR (KBr) ν cm⁻¹: 3290 (NH), 2934, 2793, 2209 (CN), 1628, 1600, 1454, 1343 (SO₂), 1177, 1158 (SO₂), 1049, 951, 752, 698, 599, 580, 547. ¹H NMR (400 MHz, DMSO-d₆) δ 8.44 (s, 1H), 7.99 (d, *J* = 8.0 Hz, 2H), 7.84 (d, *J* = 8.0 Hz, 2H), 7.20 (d, *J* = 8.0 Hz, 2H), 7.14 (d, *J* = 8.8 Hz, 2H), 3.99 (dd, *J* = 12.0, 8.0 Hz, 1H), 3.67-3.54 (m, 2H), 2.64 (s, 6H), 2.55-2.44 (m, 4H), 2.23 (b s, 2H), 1.37 (b s, 2H), 1.09 (t, *J* = 8.0 Hz, 3H). ¹³C NMR (126 MHz, DMSO-d₆) δ 161.9 (C5_{oxazole}), 147.7, 142.6, 135.1, 133.9, 129.4, 128.6, 128.3, 127.2, 125.5, 115.5, 84.4 (C4_{oxazole}), 68.6, 50.5, 44.4, 37.5, 27.7, 25.9, 24.1, 15.3. LC/MS, *m/z*: 508.2 [M+1]⁺.

4-[4-Cyano-5-(dimethylamino)-1,3-oxazol-2-yl]-*N,N*-dimethylbenzenesulfonamide **4**. Yield, 77% (colorless solid); M.p. 215-217 °C (EtOH); IR (KBr) ν cm⁻¹: 2955, 2885, 2204 (CN), 1635, 1599, 1339 (SO₂), 1161 (SO₂), 959, 940, 763, 703, 684, 593, 541. ¹H NMR (400 MHz, DMSO-d₆) δ 8.07 (d, *J* = 8.0 Hz, 2H), 7.85 (d, *J* = 8.0 Hz, 2H), 3.21 (s, 6H), 2.64 (s, 6H). ¹³C NMR (126 MHz, DMSO-d₆) δ 160.4 (C5_{oxazole}), 150.4, 148.8, 135.7, 129.2, 129.0, 128.3, 125.9, 119.6, 116.1, 115.8, 47.4, 45.9. LC/MS, *m/z*: 321.4 [M+1]⁺.

1-[4-Cyano-2-[4-(dimethylsulfamoyl)phenyl]-1,3-oxazol-5-yl]piperidine-4-carboxamide **5**. Yield, 76% (colorless solid); M.p. 240-243 °C (MeCN); IR (KBr) ν cm⁻¹: 3430-3210 (NH), 2921, 2214 (CN), 1683, 1627, 1601, 1455, 1386, 1359, 1328 (SO₂), 1306, 1250, 1199, 1155 (SO₂), 1124, 1089, 1054, 955, 932, 764, 705, 688, 585, 543. ¹H NMR (400 MHz, DMSO-d₆) δ 8.09 (d, *J* = 8.2 Hz, 2H), 7.85 (d, *J* = 8.1 Hz, 2H), 7.36 (s, 1H), 6.89 (s, 1H), 4.05 (d, *J* = 12.0 Hz, 2H), 3.28 (t, *J* = 12.0 Hz, 2H), 2.64 (s, 6H), 2.42 (t, *J* = 12.0 Hz, 2H), 1.88 (d, *J* = 12.0 Hz, 2H), 1.68 (dd, *J* = 20 Hz, 12.0 Hz, 2H). ¹³C NMR (126 MHz, DMSO-d₆) δ 175.4, 160.4 (C5_{oxazole}), 148.6, 135.6, 129.3, 128.3, 125.9, 116.0, 86.2 (C4_{oxazole}), 45.9, 37.5, 27.3. LC/MS, *m/z*: 404.0 [M+1]⁺.

4-[4-Cyano-5-(4-phenylpiperazin-1-yl)-1,3-oxazol-2-yl]-*N,N*-dimethylbenzenesulfonamide **6**. Yield, 73% (colorless solid); M.p. 196-198 °C (EtOH); IR (KBr) ν cm⁻¹: 2966, 2913, 2875, 2839, 2212 (CN), 1612, 1581, 1504, 1455, 1444, 1342 (SO₂), 1292, 1236, 1187, 1162 (SO₂), 1051, 937, 762, 703, 692, 601, 580, 544. ¹H NMR (400 MHz, DMSO-d₆) δ 8.11 (d, *J* = 8.0 Hz, 2H), 7.86 (d, *J* = 8.4 Hz, 2H), 7.26 (t, *J* = 8.0 Hz, 2H), 7.02 (d, *J* = 8.0 Hz, 2H), 6.84 (t, *J* = 8.0 Hz, 1H), 3.77 (s,

4H), 3.30 (s, 4H), 2.64 (s, 6H). ^{13}C NMR (126 MHz, DMSO- d_6) δ 160.4 ($\text{C5}_{\text{oxazole}}$), 150.4, 148.8, 135.7, 135.1, 129.2, 129.0, 128.3, 126.0, 119.6, 116.1, 115.8, 86.6 ($\text{C4}_{\text{oxazole}}$), 47.3, 45.9, 37.5. LC/MS, m/z: 438.0 $[\text{M}+1]^+$.

4-[5-(Benzylamino)-4-cyano-1,3-oxazol-2-yl]-N,N-diethylbenzenesulfonamide 7. Yield, 75% (colorless solid); M.p. 175–178 °C (EtOH); IR (KBr) ν cm^{-1} : 3381 (NH), 2980, 2207 (CN), 1629, 1603, 1583, 1451, 1352, 1332 (SO_2), 1318, 1301, 1264, 1203, 1155 (SO_2), 1086, 1045, 1016, 934, 832, 772, 734, 696, 685, 606, 566. ^1H NMR (400 MHz, DMSO- d_6) δ 9.23 (s, 1H), 7.96 (d, $J = 8.0$ Hz, 2H), 7.89 (d, $J = 8.0$ Hz, 2H), 7.40 (q, $J = 8.0$ Hz, 4H), 7.29 (t, $J = 4.0$ Hz, 1H), 4.58 (s, 2H), 3.18 (q, $J = 8.0$ Hz, 4H), 1.04 (t, $J = 8.0$ Hz, 6H). ^{13}C NMR (101 MHz, DMSO- d_6) δ 161.9 ($\text{C5}_{\text{oxazole}}$), 148.7, 140.9, 138.4, 129.6, 129.1, 128.1, 128.0, 127.9, 126.2, 115.8, 85.2 ($\text{C4}_{\text{oxazole}}$), 46.6, 42.3, 14.5. LC/MS, m/z: 411.4 $[\text{M}+1]^+$.

4-(4-Cyano-5-pyrrolidin-1-yl-1,3-oxazol-2-yl)-N,N-diethylbenzenesulfonamide 8. Yield, 65% (colorless solid); M.p. 182–184 °C (EtOH); IR (KBr) ν cm^{-1} : 2981, 2938, 2872, 2203 (CN), 1628, 1583, 1456, 1438, 1402, 1348, 1332 (SO_2), 1288, 1201, 1158 (SO_2), 1090, 1053, 1017, 954, 935, 849, 762, 735, 692, 586, 559. ^1H NMR (400 MHz, DMSO- d_6) δ 7.98 (d, $J = 8.0$ Hz, 2H), 7.89 (d, $J = 8.0$ Hz, 2H), 3.61 (q, $J = 4.0$ Hz, 4H), 3.17 (q, $J = 8.0$ Hz, 4H), 2.00 (p, $J = 4.0$ Hz, 4H), 1.04 (q, $J = 4.0$ Hz, 6H). ^{13}C NMR (126 MHz, DMSO- d_6) δ 159.0 ($\text{C5}_{\text{oxazole}}$), 148.1, 140.4, 129.0, 127.5, 125.6, 116.2, 84.4 ($\text{C4}_{\text{oxazole}}$), 48.0, 41.8, 24.9, 14.0. LC/MS, m/z: 375.2 $[\text{M}+1]^+$.

4-[5-(4-Benzylpiperazin-1-yl)-4-cyano-1,3-oxazol-2-yl]-N,N-diethylbenzenesulfonamide 9. Yield, 77% (colorless solid); M.p. 138–140 °C (EtOH); IR (KBr) ν cm^{-1} : 2213 (CN), 1629, 1621, 1347, 1335 (SO_2), 1157 (SO_2), 760, 699, 584. ^1H NMR (400 MHz, DMSO- d_6) δ 8.04 (d, $J = 8.0$ Hz, 2H), 7.89 (d, $J = 8.0$ Hz, 2H), 7.37–7.25 (m, 5H), 3.66–3.60 (m, 4H), 3.56 (d, $J = 4.0$ Hz, 2H), 3.18 (t, $J = 8.0$ Hz, 4H), 2.56 (t, $J = 8.0$ Hz, 4H), 1.04 (t, $J = 8.0$ Hz, 6H). ^{13}C NMR (126 MHz, DMSO- d_6) δ 160.4 ($\text{C5}_{\text{oxazole}}$), 158.5, 148.8, 140.8, 137.5, 128.9, 128.2, 127.5, 127.1, 126.0, 115.8, 86.3 ($\text{C4}_{\text{oxazole}}$), 61.7, 51.2, 46.1, 41.8, 14.0. LC/MS, m/z: 480.4 $[\text{M}+1]^+$.

5-(Prop-2-enylamino)-2-(4-pyrrolidin-1-ylsulfonylphenyl)-1,3-oxazole-4-carbonitrile 10. Yield, 69% (colorless solid); M.p. 201–203 °C (EtOH); IR (KBr) ν cm^{-1} : 3351 (NH), 2982, 2868, 2205 (CN), 1623, 1582, 1334 (SO_2), 1320, 1160 (SO_2), 604, 585, 570. ^1H NMR (400 MHz, DMSO- d_6) δ 8.88 (s, 1H), 7.97–7.94 (m, 4H), 6.00–5.90 (m, 1H), 5.34–5.19 (m, 2H), 4.00 (d, $J = 8.0$ Hz, 2H), 3.18–3.14 (m, 4H), 1.67–1.63 (m, 4H). ^{13}C NMR (101 MHz, DMSO- d_6) δ 161.9 ($\text{C5}_{\text{oxazole}}$), 148.7, 137.3, 134.5, 129.9, 128.7, 126.1, 117.0, 115.9, 85.1 ($\text{C4}_{\text{oxazole}}$), 48.4, 45.3, 25.2. LC/MS, m/z: 359.4 $[\text{M}+1]^+$.

5-(1,3-Benzodioxol-5-ylmethylamino)-2-(4-pyrrolidin-1-ylsulfonylphenyl)-1,3-oxazole-4-carbonitrile 11. Yield, 65% (colorless solid); M.p. 214–216 °C (EtOH); IR (KBr) ν cm^{-1} : 3353 (NH), 2977, 2868, 2202 (CN), 1625, 1601, 1501, 1442, 1335 (SO_2), 1322, 1247, 1159 (SO_2), 1040, 610, 587, 568. ^1H NMR (400 MHz, DMSO- d_6) δ 9.14 (t, $J = 6.1$ Hz, 1H), 8.00 (d, $J = 8.0$ Hz, 2H), 7.91 (d, $J = 8.0$ Hz, 2H), 6.98 (s, 1H), 6.89 (d, $J = 8.0$ Hz, 2H), 6.0 (s, 2H), 4.48 (d, $J = 8.0$ Hz, 2H), 3.18–3.15 (m, 4H), 1.68–1.60 (m, 4H). ^{13}C NMR (126 MHz, DMSO- d_6) δ 161.3 ($\text{C5}_{\text{oxazole}}$), 158.5, 148.2, 147.4, 146.6, 136.8, 131.6, 129.3, 128.1, 125.6, 120.8, 108.2, 108.0, 101.0, 84.7 ($\text{C4}_{\text{oxazole}}$), 47.8, 45.9, 24.7. LC/MS, m/z: 453.0 $[\text{M}+1]^+$.

5-[(4-Methoxyphenyl)methylamino]-2-(4-pyrrolidin-1-ylsulfonylphenyl)-1,3-oxazole-4-carbonitrile 12. Yield, 75% (colorless solid); M.p. 228–230 °C (EtOH); IR (KBr) ν cm^{-1} : 3361 (NH), 2203 (CN), 1631, 1602, 1583, 1512, 1461, 1441, 1404, 1365, 1349, 1335 (SO_2), 1319, 1286, 1245, 1190, 1177, 1157 (SO_2), 1116, 1100, 1093, 1044, 1038, 1005, 971, 855, 834, 811, 777, 697, 682, 616, 590, 572, 550, 521. ^1H NMR (400 MHz, DMSO- d_6) δ 9.17 (s, 1H), 7.99 (d, $J = 8.0$ Hz, 2H), 7.91 (d, $J = 8.0$ Hz, 2H), 7.34 (d, $J = 8.0$ Hz, 2H), 6.94 (d, $J = 8.0$ Hz, 2H), 4.50 (d, $J = 8.0$ Hz, 2H), 3.74 (s, 3H), 3.16 (m, 4H), 1.68–1.63 (m, 4H). ^{13}C NMR (126 MHz, DMSO- d_6) δ 160.4 ($\text{C5}_{\text{oxazole}}$), 158.5, 148.8, 140.8, 137.5, 128.9, 128.2, 127.5, 127.1, 126.0, 115.8, 86.3 ($\text{C4}_{\text{oxazole}}$), 61.7, 51.2, 46.1, 41.8, 14.0. LC/MS, m/z: 439.4 $[\text{M}+1]^+$.

1-[4-Cyano-2-(4-pyrrolidin-1-ylsulfonylphenyl)-1,3-oxazol-5-yl]piperidine-4-carboxamide 13. Yield, 71% colorless solid; M.p. >250 °C (MeCN); IR (KBr) ν cm^{-1} : 3408–3221 (NH), 2954, 2895, 2863, 2217 (CN), 1662, 1621, 1584, 1451, 1418, 1400, 1328 (SO_2), 1299, 1264, 1239, 1181, 1146 (SO_2), 1094, 1045, 1023, 1005, 926, 840, 774, 681, 655, 620, 586, 566. ^1H NMR (400 MHz, DMSO- d_6) δ 8.09–8.07 (d, $J = 8.0$ Hz, 2H), 7.91–7.89 (d, $J = 8.0$ Hz, 2H), 7.35 (s, 1H), 6.88 (s, 1H), 4.05 (d, $J = 16.0$ Hz, 2H), 3.34 (s, 9H), 1.88 (d, $J = 16.0$ Hz, 2H), 1.65 (d, $J = 8.0$ Hz, 4H). ^{13}C NMR (126 MHz, DMSO- d_6) δ 175.4, 160.4 ($\text{C5}_{\text{oxazole}}$), 148.6, 137.0, 129.2, 128.0, 125.9, 116.0, 86.2 ($\text{C4}_{\text{oxazole}}$), 47.8, 46.0, 40.3, 27.3, 24.7. LC/MS, m/z: 430.0 $[\text{M}+1]^+$.

5-(3,4-Dihydro-1H-isoquinolin-2-yl)-2-(4-pyrrolidin-1-ylsulfonylphenyl)-1,3-oxazole-4-carbonitrile 14. Yield, 75% (colorless solid); M.p. 219–221 °C (MeCN); IR (KBr) ν cm^{-1} : 2201 (CN), 1623, 1579, 1460, 1334 (SO_2), 1160 (SO_2), 1090, 1003, 753, 686, 601, 580. ^1H NMR (400 MHz, DMSO- d_6) δ 8.11 (d, $J = 8.0$ Hz, 2H), 7.92 (d, $J = 8.0$ Hz, 2H), 7.26 (s, 4H), 4.85 (s, 2H), 3.90 (t, $J = 8.0$ Hz, 2H), 3.17 (t, $J = 8.0$ Hz, 4H), 3.03 (t, $J = 8.0$ Hz, 2H), 1.75–1.56 (m, 4H). ^{13}C NMR (126 MHz, DMSO- d_6) δ 162.2 ($\text{C5}_{\text{oxazole}}$), 150.4, 146.8, 135.3, 129.2, 129.1, 128.3, 126.0, 116.1, 115.2, 77.4 ($\text{C4}_{\text{oxazole}}$), 75.1, 67.6, 45.9, 37.1. LC/MS, m/z: 435.4 $[\text{M}+1]^+$.

4.2. Anticancer evaluation

4.2.1. The NCI-60 one-dose assay of compounds 1-14

Novel synthesized compounds were researched at the National Cancer Institute (NCI), Bethesda, Maryland, U.S.A., by the Developmental Therapeutic Program (DTP).²⁷ The compounds were investigated using 60 human tumor cell lines of the nine cancer types: leukemia, prostate, brain, breast, lung, colon, melanoma, renal, and ovarian. The one-dose anticancer screening (10^{-5} M) was started by inoculating each line into standard 96-well microtiter plates (5000–40000 cells/well) in RPMI 1640 medium containing 5% fetal bovine serum and 2 mM L-glutamine (day 0). Next, the cells were preincubated without the drug at 37 °C and 5% CO_2 for 24 h. The studied compounds were added to the plates at a concentration of 10^{-5}

M (day 1) and incubated for 48 h at the same conditions. Then, the media were removed, and the cells were fixed in situ, washed, and dried (day 3). The sulforhodamine B assay was used for cell density determination based on the measurement of cellular protein content. After incubation, cell monolayers were fixed with trichloroacetic acid (10%) and stained for 30 min. The excess dye was removed by repeatedly washing with acetic acid (1%). The bound stain was resolubilized in Tris solution (10 mM), and optical density was measured spectrophotometrically (510 nm) on automated microplate readers.

4.2.2. The NCI-60 five-dose assay of compound 2

The five-dose (0.01, 0.1, 1, 10, and 100 μ M) growth inhibition of most activity compound **2** was evaluated against the NCI-60 total cell panel. Three dose-response parameters (GI_{50} , TGI, and LC_{50}) were calculated for each cell line. The 50% growth inhibition (GI_{50}) measures a cell's sensitivity to the drug's effect and matches the compound concentration, inducing a 50% decrease in cell growth. The TGI (total growth inhibition) is the concentration of the study drug that produces total inhibition of cell growth. The LC_{50} (cytotoxic activity) is the compound concentration causing a net 50% loss of initial cells at the end of the 48-hour incubation period. Data computations were conducted using the methods described by the NCI Development Therapeutics Program.²⁸

4.3. COMPARE analysis

The COMPARE analysis measures the degree of similarity between studied compounds and known anticancer drugs in the NCI databases. This method was developed using the Pearson correlation coefficient as a comparison criterion. The mean compound activity values graph calculates the correlation coefficient between studied compounds and standard antitumor agents with a known mechanism of action. The correlation coefficient interpretation with a standard drug was used as follows:^{29,30} insignificant $r=0.00-0.30$, weak $r=0.30-0.50$, moderate $r=0.50-0.70$, high $r=0.70-0.90$, and very high $r=0.9-1.0$. The results were quantitatively evaluated according to the Chaddock scale.³¹

4.4. Molecular docking procedure

The structures of human estrogen receptors α ($ER\alpha$) and β ($ER\beta$) were used in the docking studies. The AutoDock Tools (ADT) 1.5.6³² program prepared the protein and ligands. All polar hydrogens were added to the protein molecule, and all atoms were renumbered using the noBondOrder method. ChemAxon Marvin Sketch 5.3.735³³ software created, pre-optimized, and saved the ligand structures in Mol2 format. The optimized protein and ligands were saved in PDBQT format. The Avogadro v1.2.0 program³⁴ minimized the ligands' energy by employing the MMFF94s force field with the steepest descent algorithm. The partial charges of the ligands and protein were modified by ADT using the Gasteiger method and saved in PDBQT format. AutoDock Vina 1.1.2 program³⁵ was used for docking. The grid maps (30*30*30 points) with a grid spacing (1Å) were used. The study and visualization of protein-ligand interactions were performed by Accelrys DS 4.0.³⁶

4.5. ADMET prediction

The pkCSM Web server³⁷ has estimated the ADMET properties of compounds **2**, **3**, and **9**. This platform uses machine learning to predict the main pharmacokinetic properties of new compounds. The ADMET properties of these compounds include the main pharmacokinetic properties, such as toxicity, absorption, metabolism, elimination, and distribution.

References

- Bukowski K., Kciuk M., and Kontek, R. (2020) Mechanisms of Multidrug Resistance in Cancer Chemotherapy. *Int. J. Mol. Sci.*, 21 (9), 3233.
- Dobrydnev A.V., Tkachuk T.M., Atamaniuk V.P., and Popova M.V. (2020) Quercetin-amino acid conjugates are promising anti-cancer agents in drug discovery projects. *Mini rev. Med. Chem.*, 20 (2), 107–122.
- Ballatore C., Huryn D. M., and Smith A. B. (2013) Carboxylic acid (bio)isosteres in drug design. *ChemMedChem*, 8 (3), 385–395.
- Dobrydnev A. V., Vashchenko B. V., and Volovenko Y. M. (2018) The simplest synthesis of 5, 5-disubstituted and spiranic methyl 4-amino-2, 2-dioxo-2, 5-dihydro-1, 2 λ 6-oxathiole-3-carboxylates. *Tetrahedron let.*, 59(16), 1581-1582.
- Wani T. A., Zargar S., Alkahtani H. M., Altwaijry N., and Al-Rasheed L. S. (2023) Anticancer Potential of Sulfonamide Moieties via In-Vitro and In-Silico Approaches: Comparative Investigations for Future Drug Development. *Int. J. mol. Sci.*, 24(9), 7953.
- Popov I. O., Popova M. V., Omelian, T. V., Dobrydnev A. V., Konovalova, I. S., Shishkina, S. V., Grygorenko O. O., and Volovenko Yu. M. (2021) Reaction of dialkylaminosulfur trifluorides with β -keto sulfonamides and β -keto sulfones. *ChemistrySelect*, 6, 3084–3088.
- Cassileth P. A., and Gale R. P. (1986) Amsacrine: a review. *Leuk. Res.*, 10(11), 1257–1265.
- Poole R.M. (2014) Belinostat: First Global Approval. *Drugs*, 74, 1543–1554.

- 9 Ballantyne A. D., and Garnock-Jones K. P. (2013) Dabrafenib: first global approval. *Drugs*, 73(12), 1367–1376.
- 10 Lemjabbar-Alaoui H., Hassan O. U., Yang Y. W., and Buchanan P. (2015) Lung cancer: Biology and treatment options. *Biochim. Biophys. Acta*, 1856(2), 189–210.
- 11 Shen H., Yuan Y., Sun J., Gao W., and Shu Y. Q. (2010) Combined tamoxifen and gefitinib in non-small cell lung cancer shows antiproliferative effects. *Biomed. Pharmacother.*, 64(2), 88–92.
- 12 Shao X., Liu Y., Li Y., Xian M., Zhou Q., Yang B., Ying M., and He Q. (2016) The HER2 inhibitor TAK165 Sensitizes Human Acute Myeloid Leukemia Cells to Retinoic Acid-Induced Myeloid Differentiation by activating MEK/ERK mediated RAR α /STAT1 axis. *Sci Rep.*, 6, 24589.
- 13 Kachaeva M. V., Pilyo S. G., Demydchuk B. A., Prokopenko V. M., Zhirnov V. V., and Brovarets V. S. (2018) 4-Cyano-1, 3-oxazole-5-sulfonamides as novel promising anticancer lead compounds. *Int. J. Curr. Res.*, 10, 69410-69425.
- 14 Hogan P. J., and Cox B. G. (2009) Aqueous process chemistry: the preparation of aryl sulfonyl chlorides. *Org. Proc. Res. Dev.* 13, 875–879.
- 15 Horiuchi T., Nagata M., Kitagawa M., Akahane K., and Uoto K. (2009) Discovery of novel thieno [2, 3-d] pyrimidin-4-yl hydrazone-based inhibitors of Cyclin D1-CDK4: Synthesis, biological evaluation and structure–activity relationships. Part 2. *Bioorg. Med. Chem.*, 17(23), 7850-7860.
- 16 Havaladar F. H., and Khatri N. K. (2006) Syntheses and biological activity of 2-(4'-diethylsulfonamide phenyl)-4-substituted aminomethyl-1, 3, 4-oxadiazolin-5-thiones. *Heterocycl. Commun.*, 12(6), 453-456.

- 17 Naclerio G. A., Abutaleb N. S., Onyedibe K. I., Karanja C., Eldesouky H. E., Liang H. W., and Sintim H. O. (2022) Mechanistic studies and in vivo efficacy of an oxadiazole-containing antibiotic. *J. Med. Chem.*, 65(9), 6612-6630.
- 18 Drach B.S., Sviridov E.P., Kisilenko A.A., and Kirsanov A.V. (1973) Interaction of secondary amines with N-acyl-2,2-dichlorovinylamines and N-acyl-1-cyano-2,2-dichlorovinylamines. *J. Org. Chem. USSR (Engl. Transl.)*, 9, 1842-1846.
- 19 Najer, H., Giudicelli, R., Menin, J. (1960) *Bull. Soc. Chim.*, 2052.
- 20 Hsu L. H., Chu N. M., and Kao S. H. (2017) Estrogen, estrogen receptor and lung cancer. *Int. J. Mol. Sci.*, 18(8), 1713.
- 21 Cardoso C. M., Custódio J. B., Almeida L. M., and Moreno A. J. (2001) Mechanisms of the deleterious effects of tamoxifen on mitochondrial respiration rate and phosphorylation efficiency. *Toxicol. Appl. Pharmacol.*, 176(3), 145-152.
- 22 Kallio A., Zheng A., Dahllund J., Heiskanen K. A., and Härkönen, P. (2005) Role of mitochondria in tamoxifen-induced rapid death of MCF-7 breast cancer cells. *Apoptosis*, 10, 1395-1410.
- 23 Unten Y., Murai M., Koshitaka T., Kitao K., Shirai O., Masuya T., and Miyoshi, H. (2022) Comprehensive understanding of multiple actions of anticancer drug tamoxifen in isolated mitochondria. *Biochim. Biophys. Acta. Bioenerg.*, 1863(2), 148520.
- 24 Da Motta L. L., De Bastiani M. A., Stapenhorst F., and Klant F. (2015) Oxidative stress associates with aggressiveness in lung large-cell carcinoma. *Tumor Bio.*, 36(6), 4681-4688.
- 25 Berman H. M., Westbrook J., Feng Z., Gilliland G., Bhat T. N., Weissig H., and Bourne P. E. (2000) The protein data bank. *Nucleic. Acids. Res.*, 28(1), 235-242.
- 26 Kachaeva M. V., Hodyna D. M., Obernikhina N. V., Pilyo S. G., Kovalenko Y. S., Prokopenko V. M., and Brovarets V. S. (2019) Dependence of the anticancer activity of 1, 3-oxazole derivatives on the donor/acceptor nature of his substituents. *J. Heterocyclic Chem.*, 56(11), 3122-3134.
- 27 Boyd M. R., and Paull K. D. (1995) Some practical considerations and applications of the National Cancer Institute in vitro anticancer drug discovery screen. *Drug. Dev. Res.*, 34(2), 91-109.
- 28 Boyd M.R. (1997) *The NCI In Vitro Anticancer Drug Discovery Screen*, Humana Press, Totowa, New York.
- 29 Shoemaker R. H. (2006) The NCI60 human tumour cell line anticancer drug screen. *Nat. Rev. Cancer*, 6(10), 813-823.
- 30 Paull K. D., Shoemaker R. H., Hodes L., Monks A., Scudiero D. A., Rubinstein L., and Boyd M. R. (1989) Display and analysis of patterns of differential activity of drugs against human tumor cell lines: development of mean graph and COMPARE algorithm. *J. Natl. Cancer Inst.*, 81(14), 1088-1092.
- 31 Mukaka M. M. (2012) A guide to appropriate use of correlation coefficient in medical research. *Malawi Med. J.*, 24(3), 69-71.
- 32 Morris G. M., Huey R., Lindstrom W., Sanner M. F., Belew R. K., Goodsell D. S., and Olson, A. J. (2009) AutoDock4 and AutoDockTools4: Automated docking with selective receptor flexibility. *J. Comput. Chem.*, 30(16), 2785-2791.
- 33 ChemAxon, Marvin Sketch 5.3.735, <https://www.chemaxon.com> (assessed 05 May 2024).
- 34 Hanwell M. D., Curtis D. E., Lonie D. C., Vandermeersch T., Zurek E., and Hutchison G. R. (2012) Avogadro: an advanced semantic chemical editor, visualization, and analysis platform. *J. Cheminform.*, 4, 1-17.
- 35 Trott O., and Olson, A. J. (2010) AutoDock Vina: improving the speed and accuracy of docking with a new scoring function, efficient optimization, and multithreading. *J. Comput. Chem.*, 31(2), 455-461.
- 36 Dassault Systèmes, Discovery Studio Visualizer, <https://discover.3ds.com/> (assessed 05 May, 2024).
- Pires D. E., Blundell T. L., and Ascher D. B. (2015) pkCSM: predicting small-molecule pharmacokinetic and toxicity properties using graph-based signatures. *J. Med. Chem.*, 58(9), 4066-4072.



© 2025 by the authors; licensee Growing Science, Canada. This is an open access article distributed under the terms and conditions of the Creative Commons Attribution (CC-BY) license (<http://creativecommons.org/licenses/by/4.0/>).